의학박사학위논문

폐암세포주의 유전적 특성에 따른 페메트렉세드(pemetrexed)의 내성 기전

Resistance Mechanism to Pemetrexed According to Genetic Characteristics of Lung Cancer Cell Lines

2020 년 2 월

서울대학교 대학원

의학과 중개의학 전공

권 지 현

A Thesis of the Doctor of Philosophy Degree

Resistance Mechanism to Pemetrexed According to Genetic Characteristics of Lung Cancer Cell Lines

폐암세포주의 유전적 특성에 따른 페메트렉세드(pemetrexed)의 내성 기전

February 2020

Seoul National University College of Medicine

Department of Medicine

Translational Medicine Major

Jihyun Kwon

폐암세포주의 유전적 특성에 따른 페메트렉세드(pemetrexed)의 내성 기전

지도교수: 이 종 석

이 논문을 의학박사 학위논문으로 제출함

2019 년 10 월

서울대학교 대학원

의학과 중개의학 전공

권 지 현

권지현의 박사 학위논문을 인준함

2020 년 1월

위 원 장 김 관 민 (인)

부 위 원 장 이 종 석 (인)

위 원 정 진 행 (인)

위 원 황 진 혁 (인)

위 원 이 기 형 (인)

Abstract

Resistance Mechanism to Pemetrexed According to Genetic Characteristics of Lung Cancer Cell Lines

Jihyun Kwon

Department of Medicine

Translational Medicine Major

The Graduate School

Seoul National University

Introduction

Pemetrexed is an important therapeutic agent in the treatment of non-small cell lung cancer. Previous studies have shown that pemetrexed is more effective in cases of echinoderm microtubule-associated protein-like 4 (EML4) - anaplastic lymphoma kinase (ALK)-rearranged non-small cell lung cancer, though the mechanism remains unknown. The aim of this study was to elucidate the acquired resistance mechanisms of pemetrexed and to establish appropriate treatment strategies to overcome these resistance mechanisms. We compared the sensitivity and resistance patterns of pemetrexed in various lung cancer cell lines according to the genetic characteristics of the lung cancer.

Materials and Methods

Non-small cell lung cancer cell lines A549, NCI-H460, NCI-H2228 harboring

variant 3 type EML4-ALK rearrangement, and NCI-H3122 harboring variant 1 type EML4-ALK rearrangement were used in this experiment. Cell proliferation assay and cell cycle analysis were performed to compare the viability and the patterns of cell cycling of these cell lines after pemetrexed treatment.

We established pemetrexed-resistant sublines in A549, NCI-H460, and NCI-H3122 cell lines through exposure to increasing concentrations of pemetrexed. Colony forming assay was used to compare the proliferation capacity of parental and pemetrexed-resistant cell lines. Western blot was performed to analyze the difference in protein expression between parental and pemetrexed-resistant cell lines.

Receptor tyrosine kinase protein array and quantitative reverse transcriptase polymerase chain reaction (qRT-PCR) were performed to confirm the changes of receptor tyrosine kinase pathway-related protein expression including epidermal growth factor receptor (EGFR) and human epidermal growth factor receptor (HER) in the cells after acquisition of pemetrexed-resistance.

Based on the mechanism of pemetrexed-resistance acquisition associated with EGFR and human epidermal growth factor receptor 2 (HER2), the cells were treated with various small molecular inhibitors of this signaling pathway such as gefitinib, lapatinib, afatinib, and crizotinib and several cytotoxic agents and their survival curves were compared to find a way to overcome this resistance.

Results

EML4-ALK variant type 1-rearranged NCI-H3122 was found to be more sensitive to pemetrexed than the other cells. Cell cycle analysis after pemetrexed treatment showed that the fraction of the S phase was increased in

A549, NCI-H460 and NCI-H2228, whereas the portion of apoptotic sub-G1 increased in NCI-H3122. Subsequent experiments confirmed that pemetrexed induced apoptotic cell death early in NCI-H3122 compared to other cells.

After exposure to each cell line for about 15 months with increasing concentrations of pemetrexed, pemetrexed-resistant cell lines of A549, NCI-H460, and NCI-H3122 were established. Pemetrexed-resistant cell lines were inferior in colony forming capacity as compared to the parental cell lines.

When the expression levels of the receptor tyrosine kinase family -related protein in the parent and resistance cells were compared in each cell line, the pemetrexed-resistant NCI-H3122 cell line showed an increased expression of EGFR and HER2 compared to the parental cell line. Since this change was not dependent on the levels of EGFR ligands, it appears to be due to genetic changes in the cell.

The pan-HER inhibitor, afatinib, inhibited this alternative signaling pathway, resulting in a superior cytotoxic effect in pemetrexed-resistant NCI-H3122 cell lines than in parental cells. Afatinib also suppressed expression levels of several proteins of the receptor tyrosine kinase signaling pathway and hypoxia-inducible factor 1 alpha in pemetrexed-resistant NCI-H3122 cells, suggesting the possibility as a means to overcome resistance to pemetrexed.

Conclusion

The NCI-H3122 cell line harboring EML4-ALK variant type 1 rearrangement was more susceptible to pemetrexed-induced cell death than other cell lines. When NCI-H3122 cell lines acquire resistance to pemetrexed, the expression of EGFR and HER is increased compared to the parent cell line. These results suggest that the alternative activation of EGFR-HER signal pathways may

contribute to the acquisition of resistance to pemetrexed by non-small-cell lung cancer cells that are EML4-ALK rearrangement. Inhibition of this alternative survival signaling pathway with afatinib overcame this resistance.

Keywords : Non-small cell lung cancer; Anaplastic lymphoma kinase; Pemetrexed; Drug resistance; Afatinib

Student Number : 2012-30539

Contents

List of Tables

List of Figures

Introduction

Lung cancer is one of the most common causes of death worldwide, but recent progress in lung cancer treatment has improved its prognosis. In recent years, the use of a targeted agent has been recommended as a frontline treatment depending on the specific mutation of the cancer cells [1,2]. However, genetic mutations that could be targeted by drugs are yet to be found in more than half of lung cancer patients. In the absence of target mutations or during failure of targeted therapies, combination chemotherapy, including platinum, is generally selected as primary treatment. Among them, pemetrexed (PEM)-containing regimen is the most popular therapy, especially in adenocarcinoma patients.

PEM is a multi-targeted antifolate agent that is mainly used for malignant mesothelioma and non-small cell lung cancer (NSCLC). PEM strongly inhibits thymidylate synthase (TS), thereby interfering with folate-dependent nucleic acid synthesis and inhibiting cell division and proliferation, ultimately exhibiting antitumor effects [3,4]. The factors that predict the therapeutic response of PEM are yet to be fully understood. It is known that cancer cells with lower TS are more sensitive to PEM [5-7]. However, because PEM has various targets in addition to TS, it affects various enzymes and cell cycle regulators. Therefore, it is presumed that there are various mechanisms promoting or inhibiting the action of PEM.

Investigations have been performed to determine whether genetic mutations targeted by drugs affect the response of PEM. Some researchers have reported that the fusion of the echinoderm microtubule-associated protein–like 4 gene (EML4) with the anaplastic lymphoma kinase (ALK) gene and the reactivity to PEM are related. EML4-ALK rearrangement is found in approximately 5-10%

of NSCLC patients, especially in non-smokers and adenocarcinoma patients [8]. According to Lee et al., NSCLC patients with EML4-ALK rearrangement showed significantly higher response rates to PEM and improved progression-free survival than control patients [9]. Several studies have also shown that PEM treatment in NSCLC with EML4-ALK rearrangement is superior in response rate and survival than without this rearrangement [10-13]. These results suggest that alteration in the intracellular signaling pathway involved in ALK has a synergistic effect on the cytotoxic effect of PEM; however, the detailed mechanism is yet to be elucidated.

We identified the change in the response mechanism according to the genetic characteristics of cancer cells by observing changes in the intracellular signaling system after PEM treatment using various NSCLC cell lines, including cell lines with EML4-ALK rearrangement. In addition, we established PEM-resistant cell lines to investigate the mechanism of resistance to PEM and to discover a process to overcome this resistance.

Materials and Methods

1. Materials

Abemaciclib, adriamycin, afatinib, cisplatin, crizotinib, fluorouracil (5-FU), gefitinib, lapatinib, methotrexate (MTX), pemetrexed, and suberoylanilide hydroxamic acid (SAHA) were purchased from Selleckchem (Houston, TX, USA). The following antibodies against the following proteins were purchased from Santa Cruz Biotechnology (Dallas, TX, USA): poly (ADP-ribose) polymerase (PARP, sc-8007), Glyceraldehyde 3-phosphate dehydrogenase (GAPDH, sc-47724), and β-actin (sc-130656). Antibodies against protein kinase B (AKT, cs#4685), phospho-AKT S473 (cs#4058), phospho-AKT T308 (cs#9275), cleaved caspase-9 (cs#7237), cyclin B (cs#4138), epidermal growth factor receptor (EGFR, cs#2646), p-EGFR (cs#2236), erb-b2 receptor tyrosine kinase 2 (ERBB2/HER2, cs#2165), phospho-ERBB2 (cs#2243), ERBB3/HER3 (cs#4754), p-ERBB3/HER3 (cs#2842), mitogen-activated protein kinase (MEK, cs#13033), phospho-MEK S217/221 (cs#9154), phospho-MEK S298 (cs#98195), extracellular-signal-regulated kinase 1/2 (ERK1/2, cs#9102), p-ERK1/2 (cs#4377s), and thymidylate synthase (TS, cs#5449) were purchased from Cell Signaling Technology (Danvers, Massachusetts, USA). Mitomycin C (MMC), propidium iodide (PI), RNAse, isopropanol, and sodium dodecyl sulfate (SDS) were purchased from Sigma Aldrich (St Louis, MO, USA). Phosphatase buffer saline (PBS) and fetal bovine serum (FBS) were purchased from Gibco (Grand Island, NY, USA). Roswell Park Memorial Institute (RPMI) 1640 and Dulbecco's modified Eagle's medium (DMEM) were purchased from Welgene (Daejeon, South Korea). Human recombinant fibroblast growth factor (rhFGF) and rhEGF proteins were purchased from R&D Systems (Minneapolis, MN, USA). FITC-annexin V was

purchased from BD Biosciences (San Diego, CA, USA). All chemicals and reagents used were of analytical grade and were obtained from commercial sources.

2. Cell culture

The human A549 and NCI-H460 cells were purchased from the Korean Cell Line Bank (KCLB, Seoul, South Korea), and NCI-H2228 and NCI-H3122 cells were obtained from the American Type Culture Collection (ATCC, VA, USA). A549, NCI-H460, NCI-H2228, and NCI-H3122 cells were maintained in RPMI 1640 with 10% FBS, 4 mM L-glutamine, and 1% P/S at 37 °C with 5% CO_2. The most recent authentication of each cell line was performed using AmpFLSTR Identifiler PCR Amplification Kit (Applied Biosystems, Foster, CA, USA) by the KCLB on Nov. 12, 2019 (Table 1). A 3530xL DNA Analyzer (Applied Biosystems) and a GeneMapper v5 (Applied Biosystems) were used for DNA fingerprinting analysis.

Table 1. The DNA fingerprinting of lung cancer cell lines.

	D8S1179	D21S11	D7S820	CSF1PO	D3S1358	TH01	D13S317	D16S539	D2S1338	D19S433	Vwa	TPOX	D18S51	Amelogenin	D5S818	FGA
A549	13,14	29	8,11	10,12	16	8,9.3	11	11,12	24	13	14	8,11	14,17	X,Y	11	23
A549P	13,14	29	8,11	10,12	16	8,9.3	11	11,12	24	13	14	8,11	14,17	X,Y	11	23
A549R	13,14	29	8,11	10,12	16	8	11	11,12	24	13	14	8,11	14,17	X,Y	11	23
NCI-H460	12	30	9	11,12	15,18	9.3	13	9	17,25	14	17	8	13,15	X,Y	9,10	21,23
NCI-H460P	12	30	9,12	11,12	15,18	9.3	13	9	17,25	14	17	8	13,15	X,Y	9,10	21,23
NCI-H460R	12	30	9,12	11,12	15,18	9.3	13	9	17,25	14	17,18	8	13,16	X,Y	9,10	21,23
NCI-H3122P	13,15	28,29	8,12	11,12	16	7,9.3	10,12	11,12	17,23	14	16	10	13,16	X,Y	11,12	18,21
NCI-H3122R	13,15	28,29	8,12	11,12	16	7,9.3	10,12	11,12	17,23	14	16	10	13,16	X,Y	11,12	18,21
NCI-H2228	13	28,30	11	12	19,18	7,8	11	11,13	18	14,15	15,17	11	16	x	12	21,22

3. Cell proliferation assay

A cell proliferation assay was performed with the CellTiter-Glo Luminescent Cell Viability Assay (Promega, Madison, WI, USA) according to the manufacturer's instructions. On day 0, 96-well plates were seeded with 3,000 cells/well and incubated overnight. The next day (day 1), cells were treated with the appropriate compounds. On day 4, the plates were incubated for 1 h at room temperature and 100 μl of CellTiter-Glo reagent was added to each well, followed by mixing on an orbital shaker for 5 min. Luminescence was measured on a GloMax 96-well luminometer from Promega (Madison, WI. USA).

4. Cell Cycle Analysis

Cells were seeded in 100-mm plates and grown overnight, then subjected to the appropriate drug treatment for 24 h. After trypsinization, the cells were washed twice in PBS, fixed overnight at 4 °C in ethanol, washed three times in PBS, and incubated in PBS containing 20 μg/ml PI and 100 μg/ml RNAse at 37 °C for 30 min. After washing in PBS, cells were resuspended in 1 ml PBS and examined using a FACSCalibur flow cytometer (BD Biosciences, Franklin Lakes, NJ, USA). Cell cycle distribution was determined using FlowJo software (Tree Star, Ashland, OR, USA).

5. Western Blot Analysis

Cell lysates were clarified by centrifugation at 12,000 × *g* for 30 min at 4 °C. Protein concentration in the supernatant was measured by the Bradford assay (BioLegend, San Diego, CA, USA). Proteins (20 μg) were separated by SDS

polyacrylamide gel electrophoresis, transferred to a polyvinylidene difluoride membrane (Bio-Rad, Hercules, CA, USA) blocked in blocking buffer containing 5% skim milk, and then probed overnight with primary antibodies. Secondary antibodies conjugated with horseradish peroxidase (1:4000 dilution; Bio-Rad) were applied for 1 h. Immunoreactivity was detected by enhanced chemiluminescence (Biosesang, Seongnam, South Korea) and a ChemiDoc Touch imager (Bio-Rad).

6. Colony forming assay

Cells were seeded in 6-well plates and grown for 72 h before being subjected to the appropriate treatment for 10 days. Medium change occurred at regular time intervals. After 10 days of culture at 37 °C with 5% CO_2, colonies were washed with PBS and stained with Coomassie Brilliant Blue for 30 min at room temperature, then washed with water and air-dried. The colonies were photographed using the ChemiDoc Touch (Bio-Rad) and measured using ImageJ software (National Institutes of Health, Bethesda, MD, USA).

7. Receptor tyrosine kinase (RTK) protein array

Human RTK phosphorylation antibody array C1 kit (AAH-PRTK-1-8) and human EGFR phosphorylation array C1 kit (AAH-PER-1-4) were obtained from RayBiotech (Norcross, GA, USA). The assay for the RTK array was conducted according to the manufacturer's instructions. Lung cancer cell lysates prepared from NCI-H3122 R cells were diluted and incubated with the array's membranes. The density of the immunoreactive area obtained on the

RTK arrays was then analyzed by Chemidoc touch (Bio-Rad).

8. Quantitative reverse transcriptase polymerase chain reaction (qRT-PCR)

Total RNA was isolated from lung cancer cells using TRIzol reagent (Invitrogen Life Technologies, Grand Island, NY), following the manufacturer's instructions. RNA concentrations and purity were estimated by determining the A260/A280 ratio with a Nanodrop2000 spectrophotometer (Invitrogen). The complementary DNA (cDNA) were synthesized by cDNA Synthesis Kit (iNtRON Biotechnology, Daegu, Republic of Korea) according to the manufacturer's instructions. qRT-PCR was carried out using SYBR Green in a Thermal Cycler DiceTM Real Time System 3 (DAKARA Bio Inc). The sequences of the oligonucleotide primer were: amphiregulin (AREG) sense (5'-ATA GAG CAC CTG GAA GCA GTA ACA-3;) and antisense (5'-TGT GAG GAT CAC AGC AGA CAT AAA G-3'); betacellulin (BTC) sense (5'-CTT CAC TGT GTG GTG GCA GAT G-3') and antisense (5'-ATG CAG TAA TGC TTG TAT TGC TTG G -3'); epidermal growth factor (EGF) sense (5'-GGA CAA CAG TGC TTT GTA AAT TGT G-3;) and antisense (5'-CCA GTG TGA CTG TCT GCT TTA ACC-3'); EGFR sense (5'- TTG CCA AGG CAC GAG TAA CAA G-3;) and antisense (5'-ACT GTG TTG AGG GCA ATG AGG AC-3'); HER2 sense (5'-CTG ATG GGT TAA TGA GCA AAC TGA-3') and antisense (5'-CCA AAT TCT GTG CTG GAG GTA GAG-3'); HER3 sense (5'-GGG AGC ATT TAA TGG CAG CTA-3') and antisense (5'-GAA TGG AAT TGT CTG GGA CTG G-3'); epiregulin (EREG) sense (5'-GCT CTC AGC TGA TGT GTC CTG TA-3') and antisense (5'-AAC TGG GTT ATT ATG TGG

CCT TG-3'); heparin-binding EGF-like growth factor (HB-EGF) sense (5'-GGG CAT GAC TAA TTC CCA CTG A-3') and antisense (5'-GCC CAA TCC TAG ACG GCA AC-3'); transforming growth factor alpha (TGF-α) sense (5'-TGG CCG GGA TGG ACT AAT G-3') and antisense (5'-CTT CTG TGA CTG GGC AGG TTG-3'); and 18s sense (5'-GCT TAA TTT GAC TCA ACA CGG GA-3') and antisense (5'- AGC TAT CAA TCT GTC AAT CCT GTC-3'). The expression levels were calculated using the 2ΔΔCt method after correcting for differences in PCR efficiencies. Values were expressed relative to those of the control group.

9. RNA interference

Cells were transfected with control, ALK siRNA, EGFR siRNA, or HER2 siRNA (Bioneer, Daejeon, Republic of Korea; SN-1003, SN-238-1, SN-1956-1, or SN-2064-1, respectively) at a concentration of 100 nM using Lipofectamine 2000 reagent (Life Technologies, Carlsbad, CA, USA). After 24 h, the cells were harvested for analysis of knockdown efficiency and then were used for further analysis.

10. Statistical Analysis

Student's t-test was used to compare differences. Differences among multiple groups were evaluated by one-way analysis of variance (ANOVA) followed by Duncan's multiple range test using SPSS 23.0 software (IBM, Armonk, NY, USA). Mean values with different letters (for example, a, b, c, and d) indicate statistically significant differences ($p < 0.05$). In contrast, values having the

same letters indicate no significant differences ($p > 0.05$).

Results

1. Effect of PEM on cell viability, cell cycle, and apoptosis-associated protein expression in lung cancer cell lines

Several clinical studies have reported the potential benefits of PEM-based chemotherapy on EML4-ALK rearrangement NSCLC [14-16]. Although favorable clinical outcomes have been achieved with PEM treatment in EML4-ALK rearrangement NSCLC, it is still necessary to address the underlying mechanism.

To investigate the correlation between EML4-ALK rearrangement and PEM sensitivity, we first evaluated the protein expression of ALK in four lung cancer cell lines by western blotting. As shown in Figure 1A, ALK showed weak expression levels in the A549 and NCI-H460 cell lines. In contrast, NCI-H2228 or NCI-H3122 cells, which harbor the EML4-ALK variant (V) 3 or EML4-ALK V1 rearrangement, showed prominent protein expression of ALK. Subsequently, we determined the effect of A549, NCI-H460, NCI-H2228, and NCI-H3122 cell viability following PEM treatment (Figure 1B). The half maximal inhibitory concentration (IC50) values for PEM were 0.328 ± 0.024 nM, 0.137 ± 0.008 nM, 199.697 ± 12.522 nM, and 0.077 ± 0.015 nM in A549, NCI-H460, NCI-H2228, and NCI-H3122, respectively. Such findings indicated that NCI-H3122 cells harboring EML4-ALK V1 exhibited a greater sensitivity to PEM than the A549, NCI-H460, and NCI-H2228 with EML4-ALK V3 cell lines. Further, we showed that upon ALK knockdown with RNAi, PEM was not able to decrease cell viability in siALK NCI-H2228 and siALK NCI-H3122

cells compared to control cells (Figure 1F and 1G), indicating that the EML4-ALK rearrangement characteristics contribute to the sensitivity to PEM.

Flow cytometry analysis was performed to evaluate the effect of PEM on cell cycle transition in lung cancer cell lines (Figure 1C). PEM inhibited the progression at the S phase checkpoint to G2 phase in A549, NCI-H460, and NCI-H2228 harboring EML4-ALK V3 cells. Notably, the fraction of sub-G1 strikingly increased ($p < 0.05$), suggesting elevated apoptotic cells by PEM in NCI-H3122 cells harboring EML4-ALK V1 rearrangement.

The effect of PEM on apoptosis was examined using a caspase 3/7 activity assay. PEM (200 μM) was insufficient to cause apoptosis in A549, NCI-H460, and NCI-H2228 cells (Figure 1D). However, in NCI-H3122, caspase 3/7 activity significantly increased after PEM treatment. These results were confirmed by western blot, which revealed a strong induction of γ-H2AX, cleaved-caspase 9, and cleaved-PARP proteins after PEM treatment in a dose-dependent manner in NCI-H3122 cells compared to A549, NCI-H460, NCI-H2228 cells (Figure 1E). In A549, NCI-H460, and NCI-H2228 cells, PEM increased the protein expression of cyclin B, whereas a decreased expression of cyclin B by PEM was observed in NCI-H3122 cells. PEM also induced the protein expression of TS irrespective of EML4-ALK status among the lung cancer cell lines.

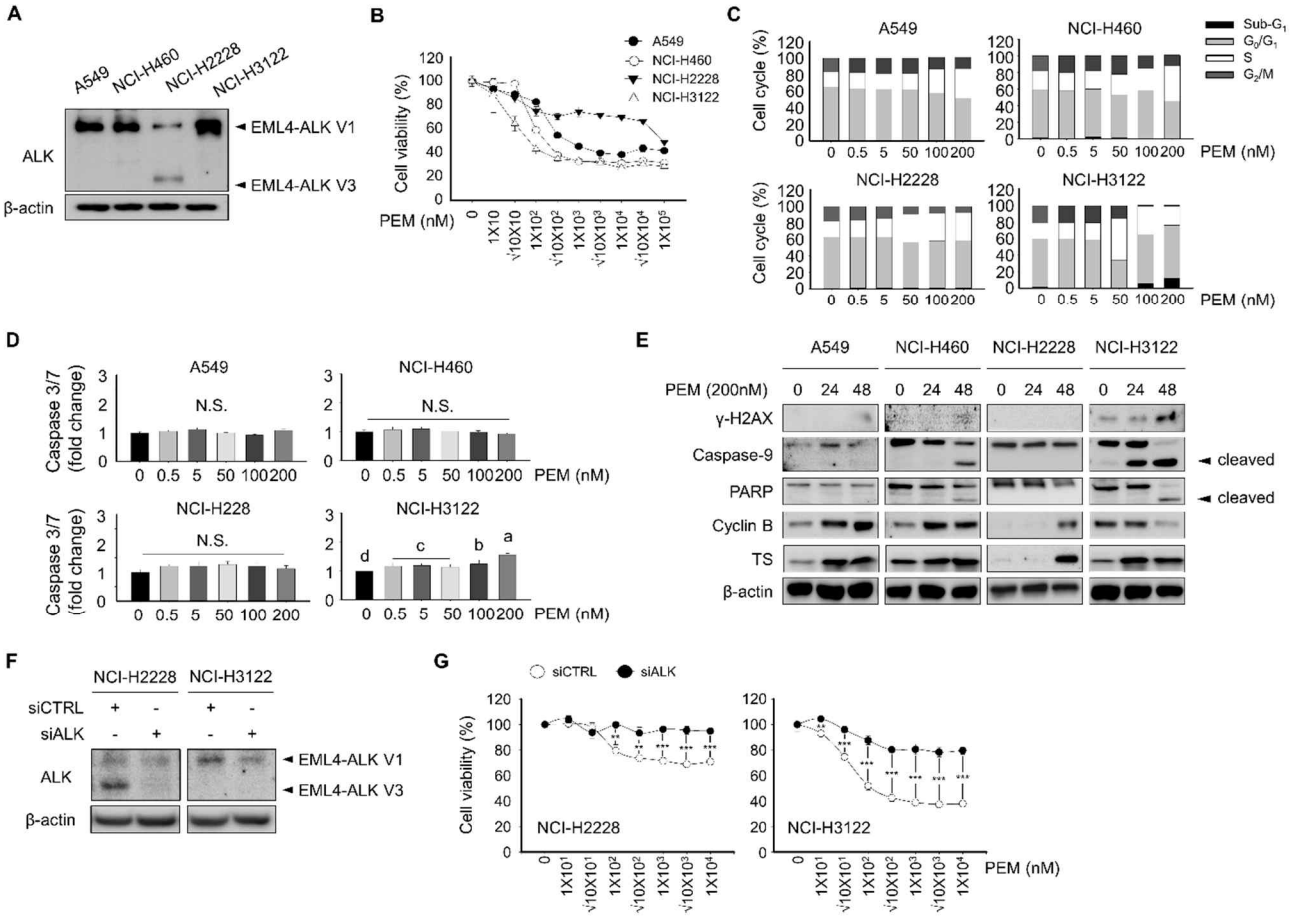
A
A549
NCI-H460
NCI-H2228
NCI-H3122
ALK
β-actin
EML4-ALK V1
EML4-ALK V3
B
A549
NCI-H460
NCI-H2228
NCI-H3122
Cell viability (%)
PEM (nM)
C
A549
NCI-H460
NCI-H2228
NCI-H3122
Sub-G1
G0/G1
S
G2/M
Cell cycle (%)
PEM (nM)
D
A549
NCI-H460
NCI-H228
NCI-H3122
Caspase 3/7 (fold change)
N.S.
PEM (nM)
E
A549
NCI-H460
NCI-H2228
NCI-H3122
PEM (200nM)
γ-H2AX
Caspase-9
PARP
Cyclin B
TS
β-actin
cleaved
F
NCI-H2228
NCI-H3122
siCTRL
siALK
ALK
β-actin
EML4-ALK V1
EML4-ALK V3
G
siCTRL
siALK
Cell viability (%)
NCI-H2228
NCI-H3122
PEM (nM)

Figure 1. Effect of PEM on cell viability, cell cycle, and apoptosis in lung cancer cell lines. A. A549, NCI-H460, NCI-H2228 EML4-ALK V3, and NCI-H3122 EML4-ALK V1 cells were evaluated for their basal expression of ALK protein by western blotting. β-actin served as the loading control. B. Cell viability assay. A549, NCI-H460, NCI-H2228, and NCI-H3122 cells were treated with the indicated concentrations of PEM for 3 days. C. Cell cycle analysis by PI staining and flow cytometry. A total of 1×10^6 cells were seeded in 60-mm plates and treated with 0, 0.5, 5, 10, 50, 100, and 200 nM of PEM for 24 h. Data are presented as histograms (black, Sub-G1; gray, G0/G1 phase; white, S phase, and dark gray, G2/M phase). D. Caspase 3/7 activity was quantified 24 h after PEM treatment in A549, NCI-H460, NCI-H2228, and NCI-H3122 cells. Means with different letters (a, b, c, and d) indicate statistically significant differences ($p < 0.05$). E. γ–H2AX, Caspase-9, PARP, cyclin B, and TS expression in A549, NCI-H460, NCI-H2228, and NCI-H3122 cells, as determined by western blotting; β-actin served as the loading control. F. Expression of ALK was evaluated using western blotting in NCI-H2228 and NCI-H3122 with or without siALK. β-Actin served as the loading control. G. Cell viability assay. NCI-H2228 and NCI-H3122 cells with or without siALK were treated with the indicated concentrations of PEM for 3 days.

2. Development of PEM-resistant lung cancer cell lines

Acquired PEM-resistant cell lines were generated by exposing A549, NCI-H460, or NCI-H3122 cells harboring EML4-ALK V1 rearrangement treated with or without 200 nM of PEM for a 15-month period (Figure 2A). After 15 months of continued exposure to 0 or 200 nM of PEM, cells became parent or resistant and were named A549 P, A549 R, NCI-H460 P, NCI-H460 R, NCI-H3122 P, and NCI-H3122 R. Cells were then cultured in the presence of 0 to 10^3 nM PEM to evaluate their PEM-acquired resistance (Figure 2B). PEM-resistant cell lines showed approximately 60% less sensitivity to PEM compared to their corresponding parental cells.

To investigate PEM resistance features, we evaluated colony formation and the cell migration ability of A549 R, NCI-H460 R, and NCI-H3122 R cells and their parental cells. Consistent with Figure 2B, PEM treatment resulted in a significantly reduced colony area in NCI-H3122 P, and lower colony density in NCI-H3122 P cells than in A549 P and NCI-H460 P cells (Figure 2C). Notably, A549 R and NCI-H460 R cells had reduced colony forming capacity compared to their parental cells. NCI-H3122 R also had a very low to nearly absent colony forming capacity.

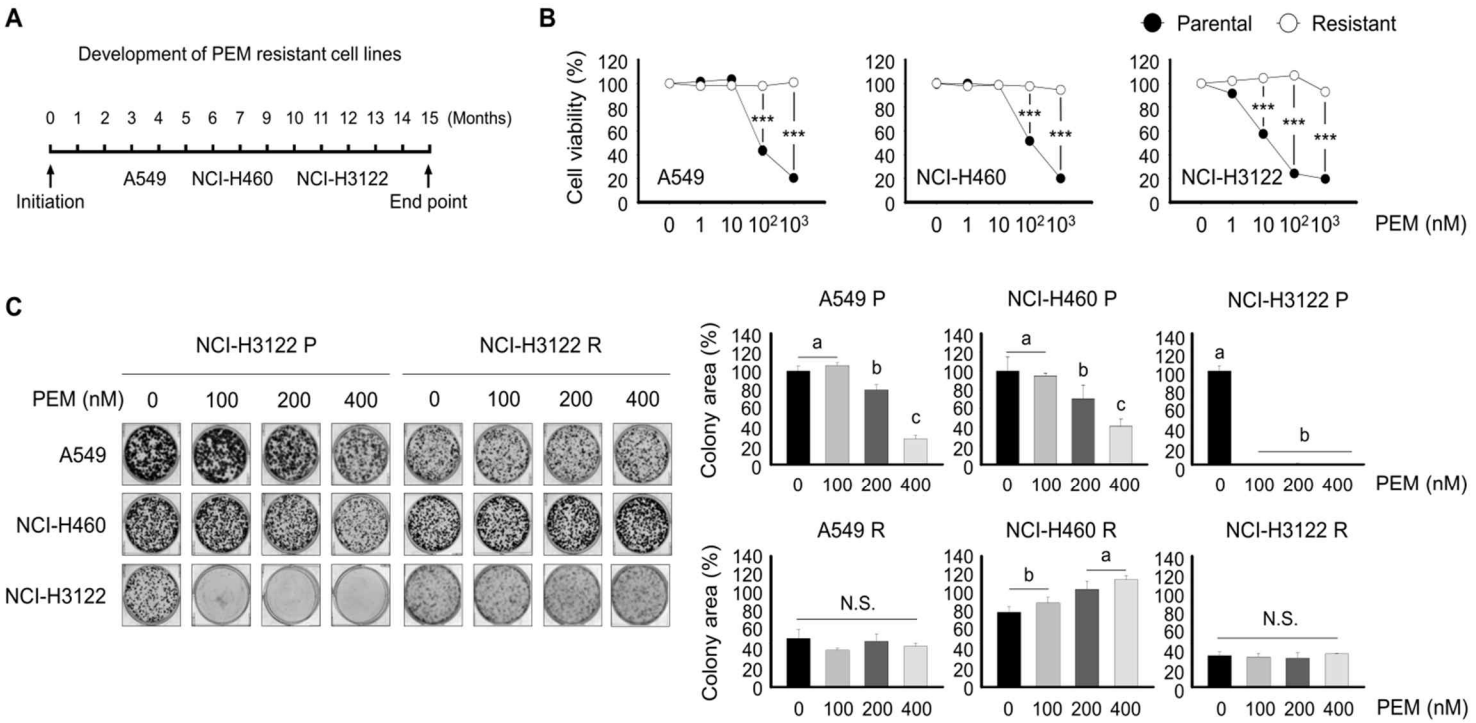

Figure 2. Development of parental and PEM-acquired resistant cell lines and evaluation of PEM sensitivity in A549, NCI-H460, and NCI-H3122 cells. A. A549, NCI-H460, and NCI-H3122 cells were treated with or without 200 nM of PEM for 15 months. B. Cell viability assays. A549 P, A549 R, NCI-H460 P, NCI-H460 R, NCI-H3122 P, and NCI-H3122 R cells were treated with the indicated concentrations of PEM for 3 days (***, $p<0.001$ versus corresponding control). C. Colony formation assays were conducted in A549 P, A549 R, NCI-H460 P, NCI-H460 R, NCI-H3122 P, and NCI-H3122 R cell lines. Means with different letters (a, b, and c) indicate statistically significant differences ($p< 0.05$; N.S., not significant).

3. Alternative activation of the RTK family as a major mechanism mediating PEM-acquired resistance

We evaluated the molecular basis of the PEM-resistance effect. Several studies have suggested that the RTK family, including EGFR, HER2, HER3, and HER4, is one of the major drug resistance mechanisms against pharmacological therapeutic reagents in different cancers, including NSCLC [17-19]. To investigate whether the activation of RTK occurs in NCI-H3122 P and NCI-H3122 R cells, we employed human RTK and EGFR phosphorylation arrays and observed that the NCI-H3122 R cell line displayed a significant increase in phospho-EGFR, EGFR, and phospho-HER2 expression compared to NCI-H3122 P (Figure 3A and 3B). An increase in the expression level of phospho-FAK, which is one of the downstream targets of EGFR and HER2 proteins, was also found in NCI-H3122 R cells.

Consistent with Figure 3A and 3B, western blotting analysis revealed that an obvious increase in the total level of EGFR protein was detected in NCI-H3122 R cells, with increased expression levels of phospho-EGFR and phospho-HER2, whereas no significant changes was observed in A549 R or NCI-H460 R cells (Figure 3C and 3D). In contrast, the expression levels of total HER3 and phospho-HER3 proteins were not altered in NCI-H3122 R cells compared to NCI-H3122 P cells (data not shown).

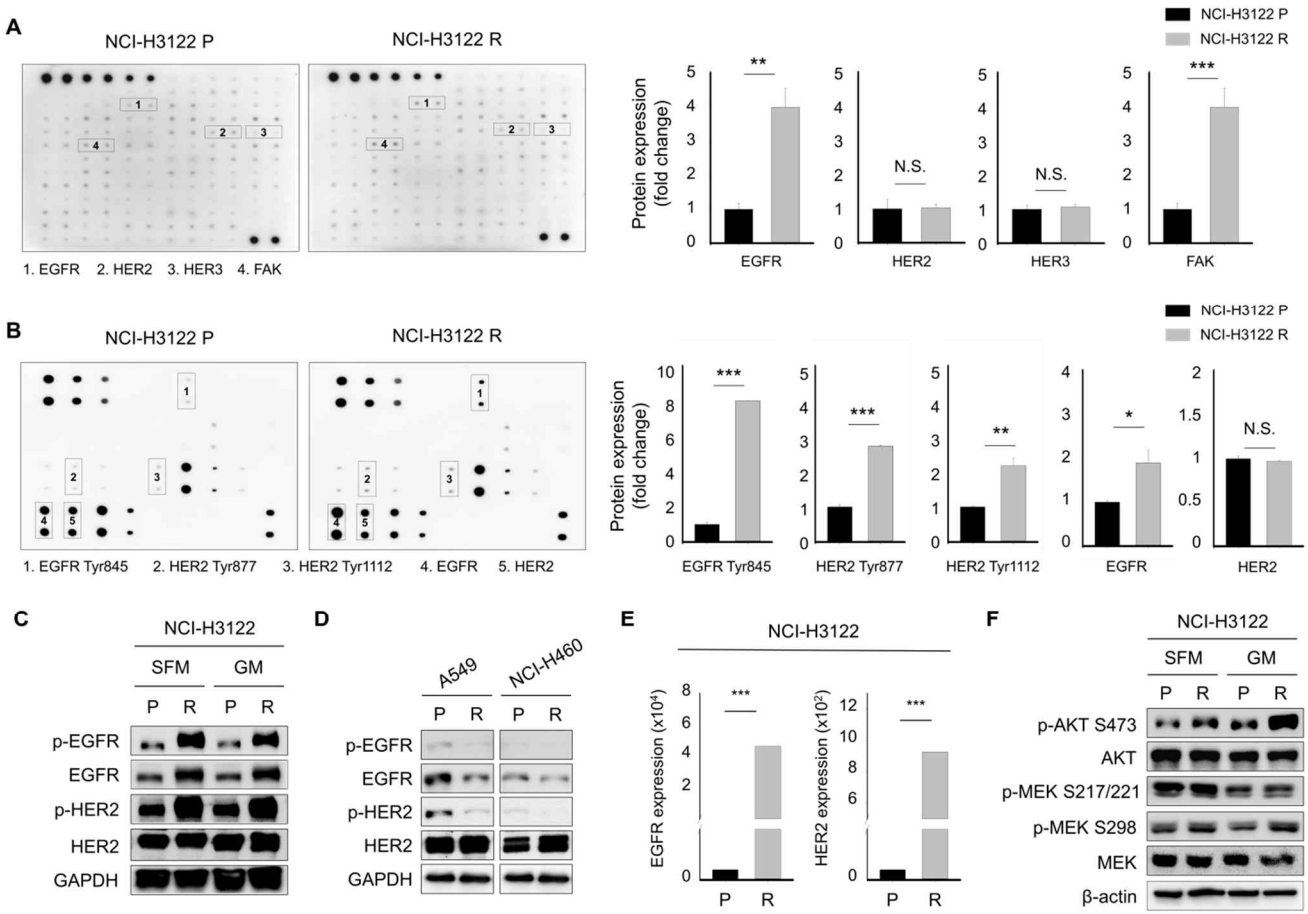
A
NCI-H3122 P
NCI-H3122 R
1. EGFR 2. HER2 3. HER3 4. FAK
NCI-H3122 P
NCI-H3122 R
Protein expression (fold change)
EGFR
HER2
HER3
FAK
N.S.
B
NCI-H3122 P
NCI-H3122 R
1. EGFR Tyr845 2. HER2 Tyr877 3. HER2 Tyr1112 4. EGFR 5. HER2
NCI-H3122 P
NCI-H3122 R
Protein expression (fold change)
EGFR Tyr845
HER2 Tyr877
HER2 Tyr1112
EGFR
HER2
N.S.
C
NCI-H3122
SFM
GM
P R P R
p-EGFR
EGFR
p-HER2
HER2
GAPDH
D
A549
NCI-H460
P R P R
p-EGFR
EGFR
p-HER2
HER2
GAPDH
E
NCI-H3122
EGFR expression (x10⁴)
HER2 expression (x10²)
P R
P R
F
NCI-H3122
SFM
GM
P R P R
p-AKT S473
AKT
p-MEK S217/221
p-MEK S298
MEK
β-actin

Figure 3. PEM-acquired resistant NSCLC cell harboring EML4-ALK rearrangement model displays overexpression of the RTK signaling pathway. A-B. RTK and EGFR phosphorylation arrays that were altered in NCI-H3122 R compared to the parental cell line. The densitometric ratio of duplicate spots for activated RTK and EGFR proteins to the internal loading controls on the RTK phosphorylation and EGFR phosphorylation array was calculated using Image J software (**, $p<0.01$; ***, $p<0.001$; N.S. not significant). C-D. Western blotting analysis of A549 P, A549 R, NCI-H460 P, NCI-H460 R, NCI-H3122 P, and NCI-H3122 R cells for phospho-EGFR, EGFR, phospho-HER2, and HER2 expression was performed. GAPDH served as the loading control (SEM, serum free media; GM; growth media). E. EGFR and HER2 mRNA expression was determined in NCI-H3122 P and NCI-H3122 R cells by qRT-PCR. Fold change in EGFR, HER2, and HER3 mRNA in NCI-H3122 R cells was compared to that in parental cells (***, $p< 0.001$; N.S. not significant). F. Western blotting analysis of NCI-H3122 P and NCI-H3122 R cells for p-AKT S473, AKT, p-MEK S217/221, p-MEK S298, and MEK. β-Actin served as the loading control (SEM, serum free media; GM; growth media).

We examined the expression levels of the mRNA of these RTKs by qRT-PCR. As a result, we found that the expression levels of EGFR and HER2 mRNA were significantly increased in NCI-H3122 R cells compared to NCI-H3122 P (Figure 3E). However, the expression level of HER3 mRNA was not altered in NCI-H3122 R cells (data not shown).

The RTK family regulates the expression levels of AKT protein [20], and the expression levels of phospho-AKT S473, phospho-MEK S217/S221, and phospho-MEK S298 protein were relatively increased in NCI-H3122 R cells compared to NCIH3122 P cells (Figure 3F).

4. Effect of acquired PEM resistance on the RTK ligands in NCI-H3122 cells

We proceeded to determine how EGFR and HER2 are activated. Previous studies suggested that the ligands of RTK secreted through the autocrine and paracrine signaling in a tumor microenvironment were the major contributors of RTK activation [21-23]. We therefore examined the expression levels of EGFR ligands including AREG, BTC, EGF, EREG, HB-EGF, and TGF-α in NCI-H3122 R cells (Figure 4A-4F). The analysis of qRT-PCR revealed that the expression levels of AREG, BTC, EGF, EREG, HB-EGF, and TGF-α were not changed in NCI-H3122 R cells compared to NCI-H3122 P cells, indicating that the expression of EGFR and HER2 is potentially activated by cellular genetic alteration in NCI-H3122 R cells.

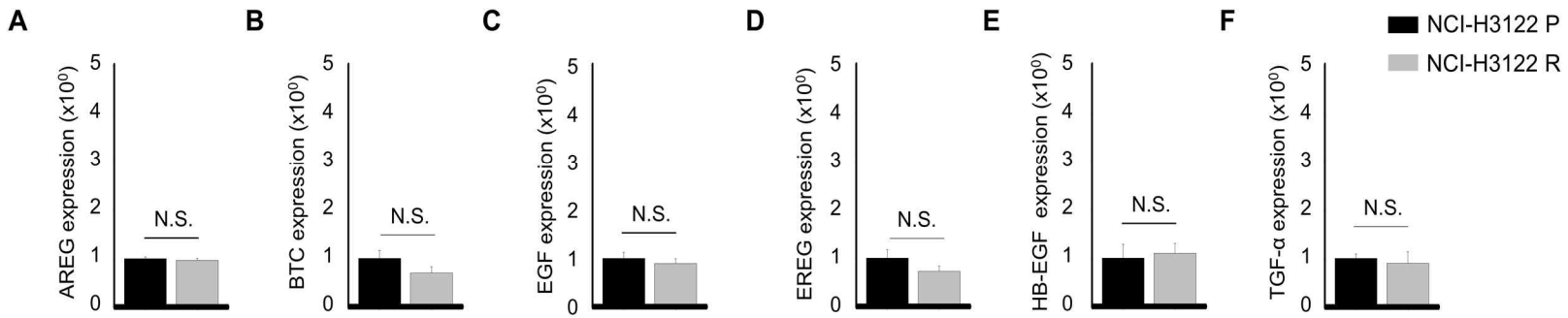

Figure 4. Effect of PEM-acquired resistance on RTK ligand mRNA expression in NCI-H3122 P and NCI-H3122 R cells. **A-F.** AREG, TRC, EGF, EREG, HB-EGF, and TGF-α mRNA expression levels were determined in NCI-H3122 P and NCI-H3122 R cells by qRT-PCR. Fold change in AREG, TRC, EGF, EREG, HB-EGF, and TGF-α mRNA in NCI-H3122 R cells was compared to that in parental cells (N.S., not significant).

5. Overcoming PEM resistance by using tyrosine kinase inhibitor (TKI)

The aforementioned evidence that NCI-H3122 R cells showed constitutive expression of EGFR and HER2 suggested that the EGFR and HER2 targeting inhibition may overcome PEM-acquired resistance.

Therefore, we first knocked down EGFR and HER2 using RNA interference in NCI-H3122 R cells and determined the transfection efficacy, a portion of apoptosis, and caspase 3/7 activity. As shown in Figure 5A, siEGFR and/or siHER2 decreased the protein expression of EGFR and/or HER2 in NCI-H3122 R cells. In addition, single EGFR or HER2 knockdown significantly increased a portion of apoptosis and caspase 3/7 activity (Figure 5B-5D). In contrast, the synergistic cell death of NCI-H3122 R cells transfected with both siEGFR and siHER2 was not observed.

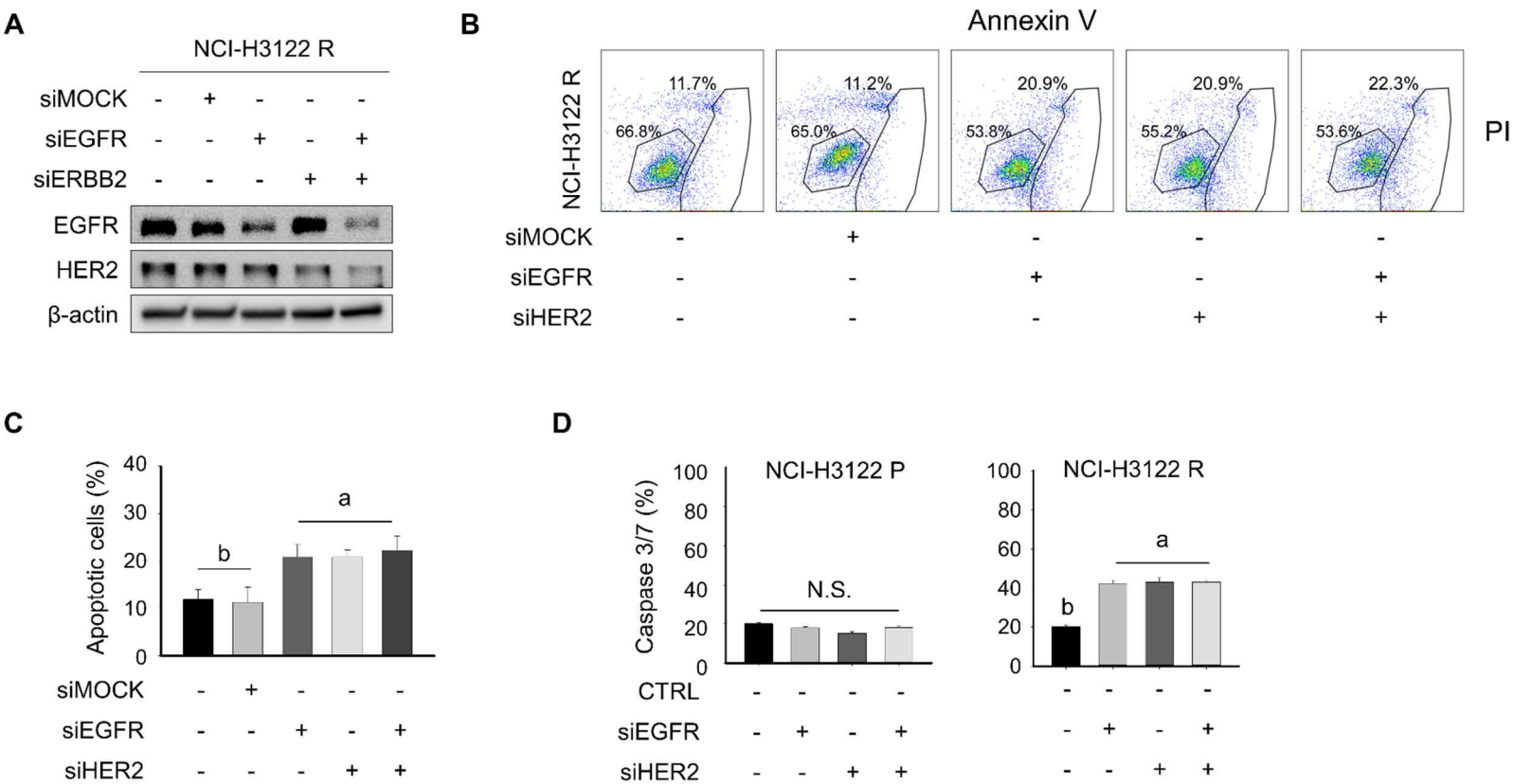
A
NCI-H3122 R
siMOCK - + - - -
siEGFR - - + - +
siERBB2 - - - + +
EGFR
HER2
β-actin
B
Annexin V
NCI-H3122 R
11.7%
66.8%
11.2%
65.0%
20.9%
53.8%
20.9%
55.2%
22.3%
53.6%
PI
siMOCK - + - - -
siEGFR - - + - +
siHER2 - - - + +
C
Apoptotic cells (%)
40
30
20
10
0
a
b
siMOCK - + - - -
siEGFR - - + - +
siHER2 - - - + +
D
Caspase 3/7 (%)
NCI-H3122 P
100
80
60
40
20
0
N.S.
NCI-H3122 R
a
b
CTRL - - - -
siEGFR - + - +
siHER2 - - + +

Figure 5. Knockdown of EGFR and/or HER2 exert a pro-apoptotic effect in NCI-H3122 R cells. **A.** NCI-H3122 R cells were transfected with siEGFR and/or siHER2 and were incubated for 24h. Cells were harvested and the expression of EGFR and HER2 was evaluated with western blotting. β-Actin served as the loading control. **B.** Apoptosis was evaluated using flow cytometry of Annexin V-PI double-stained NCI-H3122 R cells after transfection with siEGFR and/or siHER2 for 24 h. The Y-axis represents the PI-labeled population, whereas the X-axis represents the Annexin V positive cells. The left lower gating (Annexin V-, PI-) indicates normal cells, whereas the right lower gating (Annexin V+, PI-) and the right upper gating (Annexin V+, PI+) are the early and late apoptotic cells, respectively. **C.** Data are presented as histograms. Means with different letters (a and b) indicate statistically significant differences ($p < 0.05$; N.S., not significant). **D.** Caspase 3/7 activity was quantified 24 h after transfection with siEGFR and/or siHER2 in NCI-H3122 R cells. Means with different letters (a and b) indicate statistically significant differences ($p < 0.05$; N.S., not significant).

We next treated NCI-H3122 P and NCI-H3122 R cell lines with EGFR TKIs and analyzed cell viability, apoptosis, and caspase 3/7 activity. To increase the robustness of our observation, we used different EGFR TKIs such as gefitinib and afatinib. In the presence of gefitinib, cell viability and apoptotic cells were not different between the NCI-H3122 P and NCI-H3122 R cell lines (Figure 6A and 6B). Afatinib noticeably enhanced cellular sensitivity to NCI-H3122 R compared to NCI-H3122 P cells, as demonstrated by a sustained shift in IC50 value with treatment above the 100 nM afatinib concentrations. Notably, a significant increase in the incidence of apoptosis occurred with 5 and 10 μM of afatinib in NCI-H3122 R cells (Figure 6C). Concentrations of 5 and 10 μM gefitinib resulted in an insufficient number of apoptotic cells.

To confirm our findings, we performed the analysis of caspase 3/7 activity on NCI-H3122 P and NCI-H3122 R in the presence of gefitinib or afatinib (Figure 6D). Consistent with the results of cell viability and flow cytometry, increased caspase 3/7 activity was observed with afatinib in NCI-H3122 R cells.

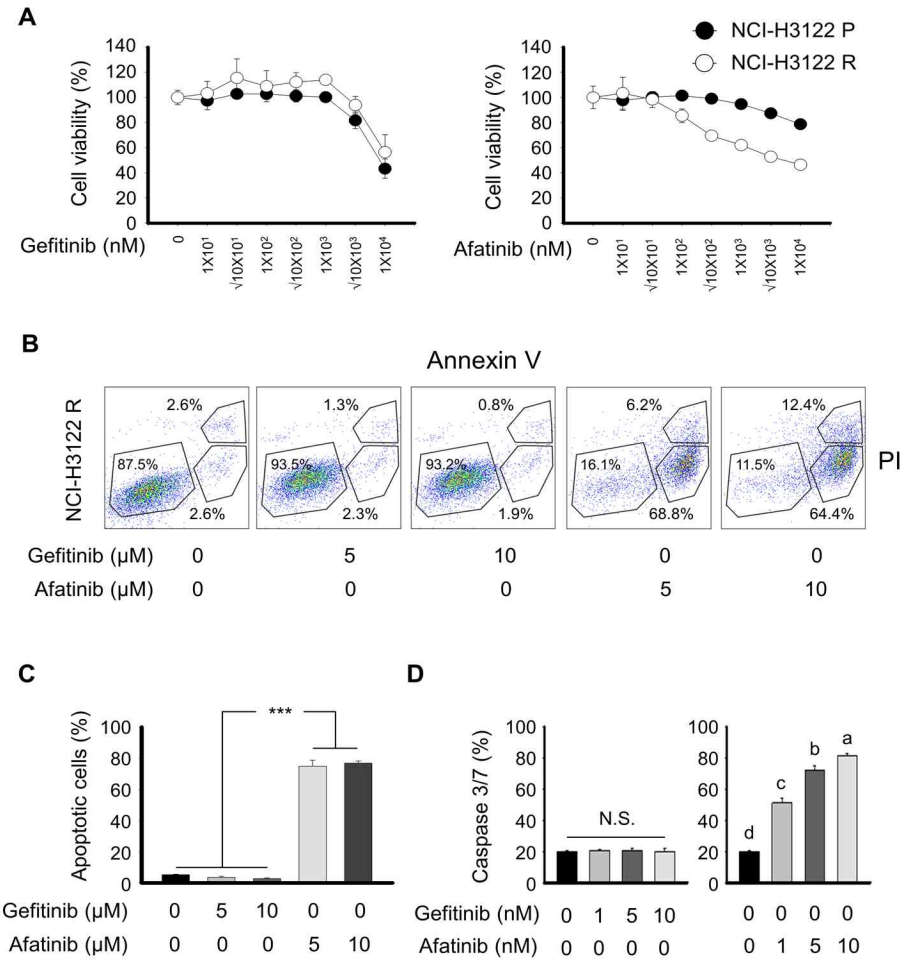

Figure 6. RTK inhibition sensitizes the acquired PEM-resistant model of NSCLC. A. NCI-H3122 P and NCI-H3122 R cells were treated with the indicated concentrations of PEM for 3 days. B. Apoptosis was evaluated by flow cytometry of Annexin V-PI double-stained NCI-H3122 R cells after treatment with gefitinib or afatinib for 24 h. The Y-axis represents the PI-labeled population, whereas the X-axis represents the Annexin V positive cells. The left lower gating (Annexin V-, PI-) indicates normal cells, whereas the right lower gating (Annexin V+, PI-) and the right upper gating (Annexin V+, PI+) are the early and late apoptotic cells, respectively. C. Data are presented as histograms (***$p < 0.001$). D. Caspase 3/7 activity (RLU, relative luminescence units) was quantified 24 h after gefitinib or afatinib in NCI-H3122 R cells. Means with different letters (a, b, c, and d) indicate statistically significant differences ($p < 0.05$; N.S., not significant).

We treated NCI-H3122 R cell lines with afatinib and PEM simultaneously and analyzed colony formation. When NCI-3122 R cells were treated with PEM and afatinib, afatinib inhibited colony formation to the same extent as cells without PEM (Figure 7A). In analysis of caspase 3/7 activity, PEM alone did not induce apoptosis of NCI-3122 R cells, but afatinib induced apoptosis regardless of the concentration of PEM (Figure 7B).

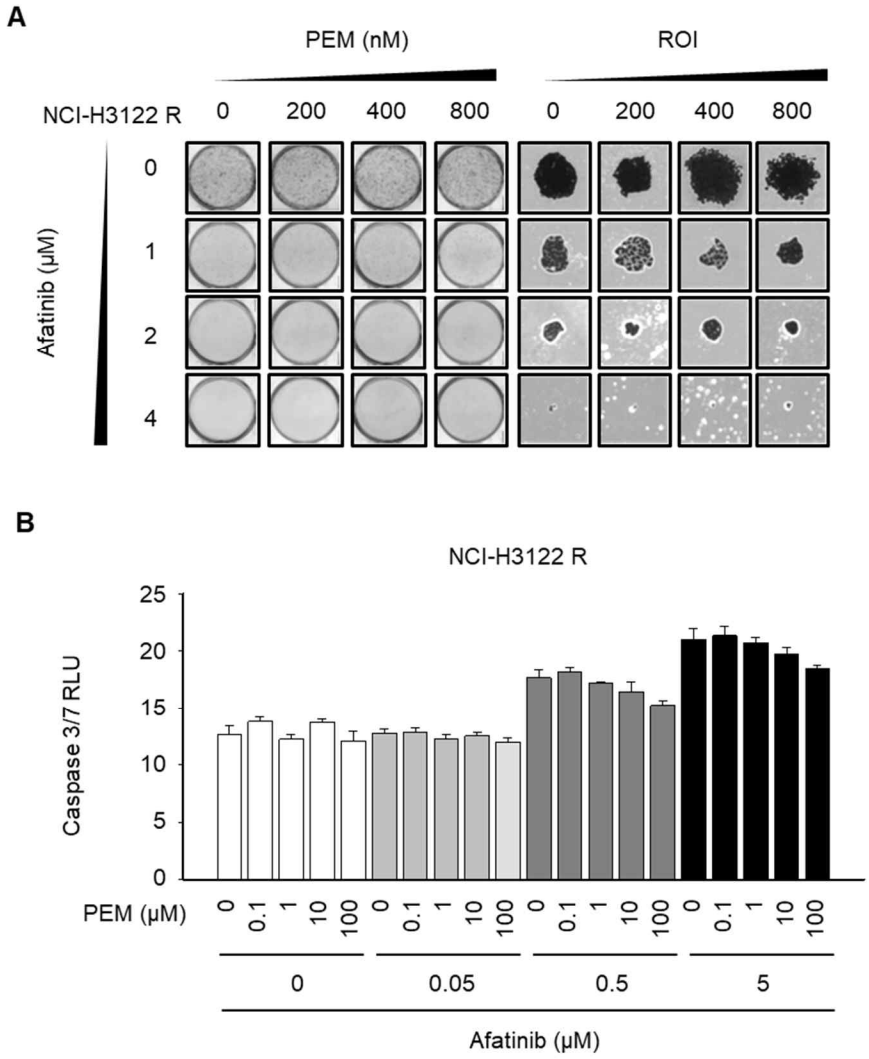

Figure 7. Effect of simultaneous PEM and afatinib treatment on NCI-H3122 cells. A. Colony forming assays were performed in NCI-H3122 R cells. B. Caspase 3/7 activity (RLU, relative luminescence units) was quantified after PEM and afatinib treatment in NCI-H3122 R cells. ROI, region of interest.

In addition, we tested other molecular inhibitors and cytotoxic agents, including lapatinib, cisplatin, methyltransferase (MTX), adriamycin, abemaciclib, SAHA, crizotinib, and fluorouracil (5-FU) whether these pharmaceutical regents could overcome PEM-acquired resistance in NCI-H3122 cells (Figure 8). These drugs have no statistically significant difference between NCI-H3122 P and NCI-H3122 R based on the IC50 values.

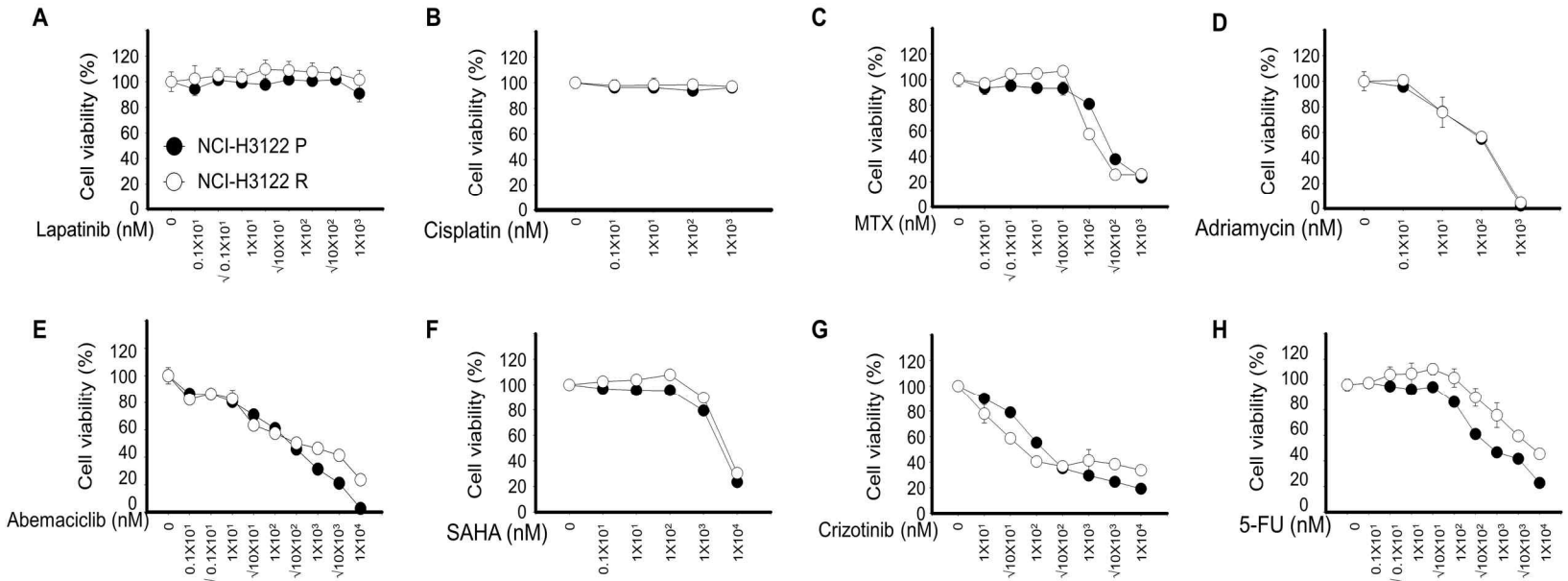

Figure 8. Effect of molecular inhibitors and cytotoxic agents on the acquisition of PEM resistance in NCI-H3122 cells. **A-H.** NCI-H3122 P and NCI-H3122 R cells were treated with the indicated concentrations of lapatinib, cisplatin, MTX, Adriamycin, abemaciclib, SAHA, crizotinib, and 5-FU for 3 days.

6. Effect of the TKIs on RTK downstream cascade and colony formation in NCI-H3122 R cells

To elucidate the underlying mechanisms involved in the overcoming TKI-mediated PEM acquired resistance, the expression levels of the RTK signaling pathway were analyzed by western blot (Figure 9A). The TKIs, afatinib and gefitinib, decreased the expression levels of phospho-EGFR and phospho-AKT S473. Furthermore, afatinib suppressed the expression levels of phospho-HER2 and phospho-MEK protein in NCI-H3122 R cells. However, gefitinib was found to be insufficient for suppressing the expression levels of phospho-HER2 and phospho-MEK protein. Hypoxia-inducible factor 1 alpha (HIF-1α) has been recognized as a gefitinib resistance molecule in NSCLC cells [24]. Interestingly, we found that the basal expression levels of the HIF-1α protein were higher in NCI-H3122 R cells that acquired resistance to PEM (Figure 9B). These data indicated that the aberrant overexpression of HIF-1α might play a partial role in PEM-acquired resistance in NSCLC cells harboring EML4-ALK rearrangements. As shown in Figure 9C, afatinib dramatically attenuated the expression level of HIF-1α in NCI-H3122 cells. In addition, colony forming assays were performed to functionally investigate the inhibitory capacity of afatinib and gefitinib in NCI-H3122 R cells. Afatinib at 1, 2, and 4 μM significantly inhibited the colony growth of NCI-H3122 R cells (Figure 9D) compared to control, but gefitinib had an ineffective potency against NCI-H3122 R cells.

Together, these data suggest that PEM-acquired resistance is strongly associated with constitutive expression of both EGFR and HER2 protein due to the potential genetic alteration, and the inhibition of those receptor activity may confer the acquired PEM resistance in NSCLC cells harboring EML4-ALK

rearrangements.

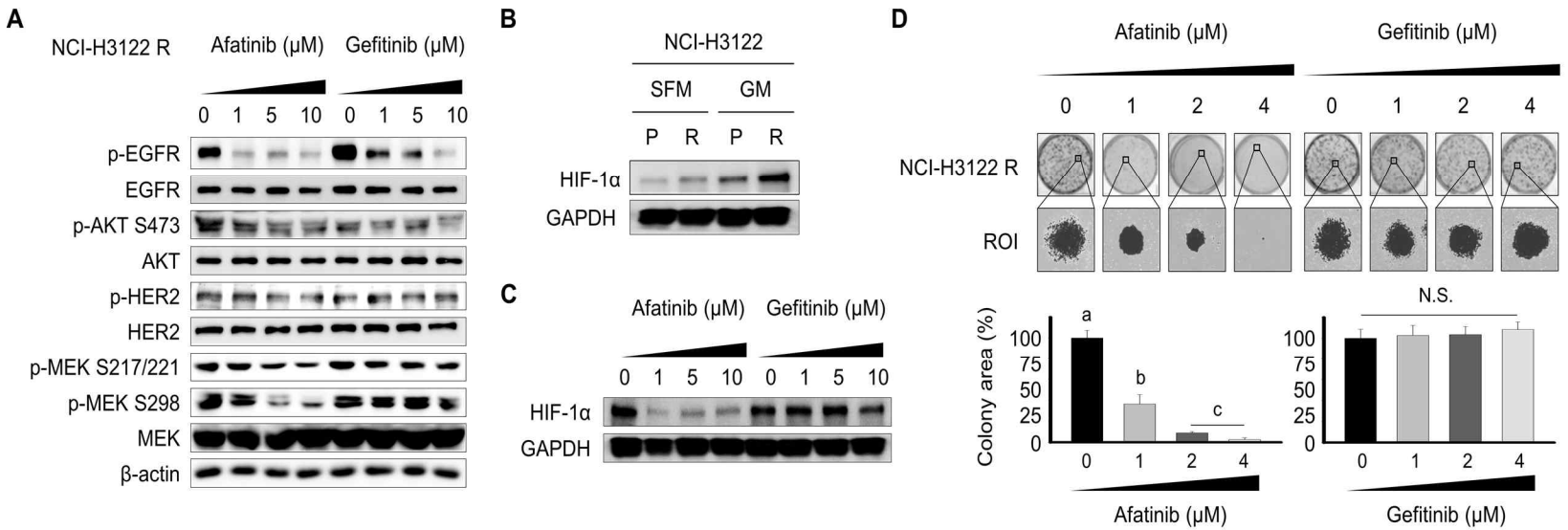

Figure 9. RTK inhibition abrogates RTK expression in NCI-H3122 R cells. A. NCI-H3122 R cells were treated with afatinib or gefitinib. The expression levels of phospho-EGFR, EGFR, phospho-AKT S473, AKT, phospho-HER2, HER2, phospho-MEK S217/221, phospho-MEK S298, and MEK were assessed by western blotting in NCI-H3122 R cells. β-actin served as the loading control. B. Basal expression of HIF-1α was evaluated by western blotting. GAPDH served as the loading control (SEM, serum free media; GM; growth media). C. NCI-H3122 R cells were treated with afatinib of gefitinib. The expression levels of HIF-1α was evaluated by western blotting in NCI-H3122 R cells. GAPDH served as the loading control. D. Colony forming assays were performed in NCI-H3122 R cells. Means with different letters (a, b, and c) indicate statistically significant differences ($p < 0.05$; N.S., not significant), ROI, region of interest.

Discussion

PEM is one of the most important cytotoxic agents used in non-squamous cell carcinoma of the lung. The main target of PEM is known as TS, but the mechanism of PEM reactivity and resistance cannot be fully explained by TS alone. It is difficult to predict the response of PEM to TS expression in tissues of real patients, and the depth and duration of responses to PEM in the same type of lung cancer vary. Several researchers have reported that NSCLC harboring EML4-ALK rearrangement is more sensitive to PEM than those with wild type ALK, but the mechanism has not been studied in depth [9-13]. The ALK receptor is a classical receptor tyrosine kinase. EML4-ALK rearrangement leads to activation of downstream signaling and contributes to cell survival and proliferation by interacting with the PI3K/AKT, JAK/STAT, and RAS/RAF/MEK/ERK [25,26]. The difference in PEM sensitivity based on the presence of ALK rearrangement suggests that PEM may have some inhibitory effects on these signaling pathways.

We found that EML4-ALK rearranged cell lines decreased their viability more rapidly during PEM treatment than wild type ALK cell lines. We also found that the superior sensitivity to PEM of EML4-ALK rearranged cells was accompanied by early onset of apoptosis during PEM treatment. Because the main mechanism of PEM is to inhibit nucleic acid synthesis, PEM alone treatment is generally known to induce S-phase arrest [27]. On the other hand, ALK inhibitors, including crizotinib, increase the sub-G1 apoptotic population in cells with the EML4-ALK rearrangement [28]. In our experiments, PEM increased the sub-G1 population, similar to crizotinib, in EML4-ALK rearranged cells, whereas S-phase arrest occurred in PEM-treated wild-type ALK cells.

Despite harboring the EML4-ALK rearrangement, the NCI-H2228 cell line had different response patterns to PEM than NCI-H3122. This is thought to result from the difference between the variant type of ALK rearrangement of NCI-H3122 and NCI-H2228. Previous studies have reported that the NCI-H2228 cell line with EML4-ALK V3 rearrangement is less sensitive to ALK inhibitors than cells with EML4-ALK V1[29]. This finding supports the notion that PEM induces apoptosis by affecting the ALK-associated signaling pathway, especially those specific to EML4-ALK V1 rearrangement and consequently exhibits an additional anti-tumor response in the EML4-ALK-rearranged cell lines. Considering the fact that PEM treatment induces the same cell cycle changes as an ALK inhibitor, and that the pattern of sensitivity according to variant type of EML4-ALK rearrangement is the same as that of an ALK inhibitor, it can be assumed that PEM works in a way similar to an ALK inhibitor in cells with the EML4-ALK rearrangement

In addition to the different reaction mechanisms for PEM, EML4-ALK rearranged cells have unique resistance mechanisms compared to ALK negative cells. In the present study, we showed that the activation of EGFR and HER family signaling accompanied by acquired PEM resistance was restricted in EML4-ALK rearranged cells. This finding suggested that the major mechanism responsible for cell survival and proliferation is the conversion from ALK association to the EGFR-HER family. It has been known that activation of the HER family-related pathway in ALK positive cells contributes to the acquisition of resistance to ALK inhibitors. Tanizaki et al. reported that blocking the ALK signaling pathway using the ALK inhibitor in EML4-ALK rearranged lung cancer cells converts cell survival from the ALK pathway-dependent mechanism to the HER family [19]. Another investigator reported the involvement of the insulin-like growth factor-1 receptor (IGF1R) and HER3

in the resistance of the next-generation ALK inhibitor, alectinib [30]. These reports suggested a hypothesis in which the increase in the levels of proteins associated with the EGFR or HER family in cells exposed to ALK inhibitors is another causative mechanism for obtaining resistance to ALK inhibitors.

In our study, EML4-ALK rearranged cells manifested an increase in HER2 activation in the presence of PEM, similar to the results of ALK inhibitors in the previous studies. This finding suggests that PEM activates the HER pathway similar to ALK inhibitors, which leads to the development of resistance to PEM. Consistent with our results, Wang et al. reported that the efficacy of PEM-containing chemotherapy was most pronounced in NSCLC harboring ALK rearrangement or ROS1 mutations, whereas NSCLC with HER mutations was poorly responsive to PEM treatment [31]. Given these results, it can be assumed that activation of the HER signal pathway may play a role in acquiring PEM resistance. In addition, PEM-resistant and parental cell lines showed no difference in responsiveness to crizotinib. We therefore assumed that PEM has an inhibitory effect on ALK signaling, but the target of PEM is a component of the downstream signaling pathway, and not of ALK itself.

Given that the development of resistance to PEM in ALK positive cells is associated with the activation of the alternative signaling system, including the HER family, this leads to the possibility that EGFR-HER inhibition will have a therapeutic effect on lung cancer that has acquired PEM resistance. Previous studies have shown that intracellular changes by PEM are associated with responsiveness to EGFR-HER inhibitors. Li et al. reported the use of the EGFR inhibitor, erlotinib, after PEM was deemed effective in ALK wild type NSCLC cells [32]. They reported that PEM increases the phosphorylation of EGFR and AKT, and blocking PEM-activated EGFR-dependent PIK3-AKT pathway with

erlotinib after PEM treatment may provide additional cytotoxicity. This finding was observed regardless of EGFR and KRAS mutations. Although conducted using NSCLC cells without ALK rearrangement, this study provides a clue to the fact that intracellular changes by PEM are related to the EGFR signaling system and the utility of a treatment strategy using EGFR inhibitors after PEM.

In our experiments, the pan-HER inhibitor afatinib had no effect on EML4-ALK-rearranged parental cells, but its cytotoxic activity increased after obtaining PEM resistance. The EGFR inhibitor gefitinib was ineffective because various HER molecules in addition to EGFR may contribute to PEM reactivity and resistance in ALK-positive cells. These findings suggest that the inhibition of several HER molecules is required to overcome the survival inhibitory effect by PEM in EML4-ALK rearranged cells.

We also showed that the acquisition of PEM resistance was accompanied by overexpression of HIF-1α protein. HIF-1α is a factor that is activated in a hypoxic state to regulate cell survival and apoptosis, and is known to mainly have an anti-apoptotic function [33]. Another reason for not responding to gefitinib despite the increased expression of EGFR in PEM-resistant cell lines may be the activation of HIF-1α by PEM. Our study showed that afatinib, on the other hand, attenuate the increased levels of HIF-1α in PEM-resistant cell lines. Therefore, we suggest that the pan-HER inhibitor may be a more appropriated therapeutic option for NSCLC with EML4-ALK rearrangement after prolonged exposure to PEM, even it has not been initially identified as having HER overexpression. Further experiments are needed in the future for the development of a clinically useful treatment strategy.

Our research has some limitations. Because the experiments here involved typical non-small-cell lung cancer cell lines, the mechanisms in the tissues of

actual patients with lung cancer may be different or more complex than those found here. In addition, the concentration of PEM used to establish resistant cell lines is much higher than the concentration of the drug present in the lung tissue of patients treated with PEM in actual clinical practice. Therefore, the real mechanism of resistance to PEM may not necessarily be identical to the results of our experiment, so care must be taken when interpreting the data here and applying it clinically.

Nevertheless, we found that the activation of the EGFR-HER2 signaling pathway was specifically involved in building PEM resistance in EML4-ALK rearrangement-positive cell lines, finding also that therapies targeting this pathway may have clinical utility. Indeed, we found that among several TKIs, afatinib can have additional therapeutic effects on ALK-rearranged NSCLC in cases where PEM resistance has developed. Although there are relatively few NSCLC patients who show evidence of EML4-ALK rearrangement, our data may have some significance if the results here can lead to changes in clinical practices. In future studies, we will attempt to elucidate mechanisms and approaches capable of overcoming PEM primary resistance in NSCLC cases without EML4-ALK rearrangement.

References

1. Ettinger, D.S.; Aisner, D.L.; Wood, D.E.; Akerley, W.; Bauman, J.; Chang, J.Y.; Chirieac, L.R.; D'Amico, T.A.; Dilling, T.J.; Dobelbower, M., et al. NCCN Guidelines Insights: Non-Small Cell Lung Cancer, Version 5.2018. J Natl Compr Canc Netw 2018, 16, 807-821, doi:10.6004/jnccn.2018.0062.

2. Hanna, N.; Johnson, D.; Temin, S.; Masters, G. Systemic Therapy for Stage IV Non-Small-Cell Lung Cancer: American Society of Clinical Oncology Clinical Practice Guideline Update Summary. J Oncol Pract 2017, 13, 832-837, doi:10.1200/JOP.2017.026716.

3. Shih, C.; Chen, V.J.; Gossett, L.S.; Gates, S.B.; MacKellar, W.C.; Habeck, L.L.; Shackelford, K.A.; Mendelsohn, L.G.; Soose, D.J.; Patel, V.F., et al. LY231514, a pyrrolo[2,3-d]pyrimidine-based antifolate that inhibits multiple folate-requiring enzymes. Cancer Res 1997, 57, 1116-1123.

4. Baldwin, C.M.; Perry, C.M. Pemetrexed: a review of its use in the management of advanced non-squamous non-small cell lung cancer. Drugs 2009, 69, 2279-2302, doi:10.2165/11202640-000000000-00000.

5. Scagliotti, G.; Hanna, N.; Fossella, F.; Sugarman, K.; Blatter, J.; Peterson, P.; Simms, L.; Shepherd, F.A. The differential efficacy of pemetrexed according to NSCLC histology: a review of two Phase III studies. Oncologist 2009, 14, 253-263, doi:10.1634/theoncologist.2008-0232.

6. Hashimoto, H.; Ozeki, Y.; Sato, M.; Obara, K.; Matsutani, N.; Nakagishi, Y.; Ogata, T.; Maehara, T. Significance of thymidylate synthase gene expression level in patients with adenocarcinoma of the lung. Cancer 2006, 106,

1595-1601, doi:10.1002/cncr.21777.

7. Ceppi, P.; Volante, M.; Saviozzi, S.; Rapa, I.; Novello, S.; Cambieri, A.; Lo Iacono, M.; Cappia, S.; Papotti, M.; Scagliotti, G.V. Squamous cell carcinoma of the lung compared with other histotypes shows higher messenger RNA and protein levels for thymidylate synthase. Cancer 2006, 107, 1589-1596, doi:10.1002/cncr.22208.

8. Shaw, A.T.; Yeap, B.Y.; Mino-Kenudson, M.; Digumarthy, S.R.; Costa, D.B.; Heist, R.S.; Solomon, B.; Stubbs, H.; Admane, S.; McDermott, U., et al. Clinical features and outcome of patients with non-small-cell lung cancer who harbor EML4-ALK. J Clin Oncol 2009, 27, 4247-4253, doi:10.1200/JCO.2009.22.6993.

9. Lee, J.O.; Kim, T.M.; Lee, S.H.; Kim, D.W.; Kim, S.; Jeon, Y.K.; Chung, D.H.; Kim, W.H.; Kim, Y.T.; Yang, S.C., et al. Anaplastic lymphoma kinase translocation: a predictive biomarker of pemetrexed in patients with non-small cell lung cancer. J Thorac Oncol 2011, 6, 1474-1480, doi:10.1097/JTO.0b013e3182208fc2.

10. Lee, H.Y.; Ahn, H.K.; Jeong, J.Y.; Kwon, M.J.; Han, J.H.; Sun, J.M.; Ahn, J.S.; Park, K.; Choi, Y.L.; Ahn, M.J. Favorable clinical outcomes of pemetrexed treatment in anaplastic lymphoma kinase positive non-small-cell lung cancer. Lung Cancer 2013, 79, 40-45, doi:10.1016/j.lungcan.2012.10.002.

11. Camidge, D.R.; Kono, S.A.; Lu, X.; Okuyama, S.; Baron, A.E.; Oton, A.B.; Davies, A.M.; Varella-Garcia, M.; Franklin, W.; Doebele, R.C. Anaplastic lymphoma kinase gene rearrangement in non-small cell lung cancer are associated with prolonged progression-free survival on pemetrexed. J Thorac Oncol 2011, 6, 774-780, doi:10.1097/JTO.0b013e31820cf053.

12. Park, S.; Park, T.S.; Choi, C.M.; Lee, D.H.; Kim, S.W.; Lee, J.S.; Kim, W.S.; Song, J.S.; Lee, J.C. Survival Benefit of Pemetrexed in Lung Adenocarcinoma Patients With Anaplastic Lymphoma Kinase Gene Rearrangement. Clin Lung Cancer 2015, 16, e83-89, doi:10.1016/j.cllc.2015.01.003.

13. Park, S.; Kim, H.J.; Choi, C.M.; Lee, D.H.; Kim, S.W.; Lee, J.S.; Kim, W.S.; Choi, S.H.; Rho, J.K.; Lee, J.C. Predictive factors for a long-term response duration in non-squamous cell lung cancer patients treated with pemetrexed. BMC Cancer 2016, 16, 417, doi:10.1186/s12885-016-2457-0.

14. Shaw, A.T.; Varghese, A.M.; Solomon, B.J.; Costa, D.B.; Novello, S.; Mino-Kenudson, M.; Awad, M.M.; Engelman, J.A.; Riely, G.J.; Monica, V., et al. Pemetrexed-based chemotherapy in patients with advanced, ALK-positive non-small cell lung cancer. Ann Oncol 2013, 24, 59-66, doi:10.1093/annonc/mds242.

15. Solomon, B.J.; Mok, T.; Kim, D.W.; Wu, Y.L.; Nakagawa, K.; Mekhail, T.; Felip, E.; Cappuzzo, F.; Paolini, J.; Usari, T., et al. First-line crizotinib versus chemotherapy in ALK-positive lung cancer. N Engl J Med 2014, 371, 2167-2177, doi:10.1056/NEJMoa1408440.

16. Solomon, B.J.; Kim, D.W.; Wu, Y.L.; Nakagawa, K.; Mekhail, T.; Felip, E.; Cappuzzo, F.; Paolini, J.; Usari, T.; Tang, Y., et al. Final Overall Survival Analysis From a Study Comparing First-Line Crizotinib Versus Chemotherapy in ALK-Mutation-Positive Non-Small-Cell Lung Cancer. J Clin Oncol 2018, 36, 2251-2258, doi:10.1200/JCO.2017.77.4794.

17. Kim, S.; Kim, T.M.; Kim, D.W.; Kim, S.; Kim, M.; Ahn, Y.O.; Keam, B.; Heo, D.S. Acquired Resistance of MET-Amplified Non-small Cell Lung

Cancer Cells to the MET Inhibitor Capmatinib. Cancer Res Treat 2019, 51, 951-962, doi:10.4143/crt.2018.052.

18. Logue, J.S.; Morrison, D.K. Complexity in the signaling network: insights from the use of targeted inhibitors in cancer therapy. Genes Dev 2012, 26, 641-650, doi:10.1101/gad.186965.112.

19. Tanizaki, J.; Okamoto, I.; Okabe, T.; Sakai, K.; Tanaka, K.; Hayashi, H.; Kaneda, H.; Takezawa, K.; Kuwata, K.; Yamaguchi, H., et al. Activation of HER family signaling as a mechanism of acquired resistance to ALK inhibitors in EML4-ALK-positive non-small cell lung cancer. Clin Cancer Res 2012, 18, 6219-6226, doi:10.1158/1078-0432.CCR-12-0392.

20. Manning, B.D.; Toker, A. AKT/PKB Signaling: Navigating the Network. Cell 2017, 169, 381-405, doi:10.1016/j.cell.2017.04.001.

21. Kimura, M.; Endo, H.; Inoue, T.; Nishino, K.; Uchida, J.; Kumagai, T.; Kukita, Y.; Kato, K.; Imamura, F.; Inoue, M. Analysis of ERBB ligand-induced resistance mechanism to crizotinib by primary culture of lung adenocarcinoma with EML4-ALK fusion gene. J Thorac Oncol 2015, 10, 527-530, doi:10.1097/JTO.0000000000000381.

22. Yamada, T.; Takeuchi, S.; Nakade, J.; Kita, K.; Nakagawa, T.; Nanjo, S.; Nakamura, T.; Matsumoto, K.; Soda, M.; Mano, H., et al. Paracrine receptor activation by microenvironment triggers bypass survival signals and ALK inhibitor resistance in EML4-ALK lung cancer cells. Clin Cancer Res 2012, 18, 3592-3602, doi:10.1158/1078-0432.CCR-11-2972.

23. Renne, C.; Willenbrock, K.; Kuppers, R.; Hansmann, M.L.; Brauninger, A. Autocrine- and paracrine-activated receptor tyrosine kinases in classic Hodgkin lymphoma. Blood 2005, 105, 4051-4059, doi:10.1182/blood-

2004-10-4008.

24. Meng, S.; Wang, G.; Lu, Y.; Fan, Z. Functional cooperation between HIF-1alpha and c-Jun in mediating primary and acquired resistance to gefitinib in NSCLC cells with activating mutation of EGFR. Lung Cancer 2018, 121, 82-90, doi:10.1016/j.lungcan.2018.04.024.

25. Hallberg, B.; Palmer, R.H. The role of the ALK receptor in cancer biology. Ann Oncol 2016, 27 Suppl 3, iii4-iii15, doi:10.1093/annonc/mdw301.

26. Sabir, S.R.; Yeoh, S.; Jackson, G.; Bayliss, R. EML4-ALK Variants: Biological and Molecular Properties, and the Implications for Patients. Cancers (Basel) 2017, 9, doi:10.3390/cancers9090118.

27. Chattopadhyay, S.; Moran, R.G.; Goldman, I.D. Pemetrexed: biochemical and cellular pharmacology, mechanisms, and clinical applications. Mol Cancer Ther 2007, 6, 404-417, doi:10.1158/1535-7163.MCT-06-0343.

28. Hamedani, F.S.; Cinar, M.; Mo, Z.; Cervania, M.A.; Amin, H.M.; Alkan, S. Crizotinib (PF-2341066) induces apoptosis due to downregulation of pSTAT3 and BCL-2 family proteins in NPM-ALK(+) anaplastic large cell lymphoma. Leuk Res 2014, 38, 503-508, doi:10.1016/j.leukres.2013.12.027.

29. Koivunen, J.P.; Mermel, C.; Zejnullahu, K.; Murphy, C.; Lifshits, E.; Holmes, A.J.; Choi, H.G.; Kim, J.; Chiang, D.; Thomas, R., et al. EML4-ALK fusion gene and efficacy of an ALK kinase inhibitor in lung cancer. Clin Cancer Res 2008, 14, 4275-4283, doi:10.1158/1078-0432.CCR-08-0168.

30. Isozaki, H.; Ichihara, E.; Takigawa, N.; Ohashi, K.; Ochi, N.; Yasugi, M.; Ninomiya, T.; Yamane, H.; Hotta, K.; Sakai, K., et al. Non-Small Cell Lung Cancer Cells Acquire Resistance to the ALK Inhibitor Alectinib by Activating Alternative Receptor Tyrosine Kinases. Cancer Res 2016, 76, 1506-1516,

doi:10.1158/0008-5472.CAN-15-1010.

31. Wang, Y.; Zhang, S.; Wu, F.; Zhao, J.; Li, X.; Zhao, C.; Ren, S.; Zhou, C. Outcomes of Pemetrexed-based chemotherapies in HER2-mutant lung cancers. BMC Cancer 2018, 18, 326, doi:10.1186/s12885-018-4277-x.

32. Li, T.; Ling, Y.H.; Goldman, I.D.; Perez-Soler, R. Schedule-dependent cytotoxic synergism of pemetrexed and erlotinib in human non-small cell lung cancer cells. Clin Cancer Res 2007, 13, 3413-3422, doi:10.1158/1078-0432.CCR-06-2923.

33. Greijer, A.E.; van der Wall, E. e role of hypoxia inducible factor 1 (HIF-1) in hypoxia induced apoptosis. J Clin Pathol 2004, 57, 1009-1014, doi:10.1136/jcp.2003.015032.

요약(국문초록)

폐암세포주의 유전적 특성에 따른 페메트렉세드(pemetrexed)의 내성 기전

권지현

의학과 중개의학 전공

서울대학교 의과대학

서론: 페메트렉세드는 비소세포폐암의 치료에 매우 중요한 항암제이다. 이전에 일부 연구자들은 적혈구 미세 소관 관련 단백질 유사 4 (EML4)-역형성 림프종 키나제 (ALK) 재배열이 있는 비소세포폐암에서 페메트렉세드의 치료 효과가 더 우월하다는 결과를 보고한 바 있다. 이 연구의 목적은 비소세포폐암에서 페메트렉세드에 대한 내성을 획득하는 기전을 규명하고, 이를 극복하는 방법을 개발함으로써 향후 임상적인 유용성을 평가하고자 하는 것이다. 이 연구에서는 여러 가지 비소세포폐암 세포주를 이용하여, 각 세포주가 가지고 있는 다양한 유전적 특성에 따른 페메트렉세드의 민감도와 내성 획득 양상의 차이를 분석하였다.

연구방법: EML4-ALK variant 1 재배열이 있는 폐선암 세포인

NCI-H3122 세포주와 EML4-ALK variant 3 재배열이 있는 NCI-H2228 세포주, 그리고 EML4-ALK 재배열이 없는 비소세포폐암 세포주인 A549와 NCI-H460이 실험에 이용되었다. 각 세포주에 페메트렉세드를 처리한 후 세포의 생존 양상을 비교하고 세포 주기를 분석함으로써 페메트렉세드에 대한 각 세포주의 민감도와 반응 기전을 평가하였다.

또한 A549, NCI-H460 및 NCI-H3122 세포주를 페메트렉세드의 농도를 점차 증가시켜가면서 장기간 노출시켜 배양함으로써 각각의 페메트렉세드-내성 세포주를 확립하였다. 만들어진 내성 세포주와 부모 세포주에 페메트렉세드를 처리한 후 세포의 생장 곡선을 비교하여 내성 발생을 확인하였으며, 부모 세포주와 내성 세포주의 증식 능력을 비교하기 위해 콜로니 생성 능력을 평가하였다. 또한 페메트렉세드 내성 획득 후 세포 내의 표피 성장 인자 수용체 (epidermal growth factor receptor, EGFR), 사람 표피 성장인자 (human epidermal growth factor receptor, HER) 관련 신호전달체계를 비롯한 각종 요소의 발현 변화를 확인하기 위해, 내성 세포주와 부모 세포주에 대해 웨스턴 블롯, 수용체 티로신 키나제 단백질 어레이 및 정량적 역전사 중합효소 연쇄반응을 시행하였다.

페메트렉세드 내성 획득에 관여하는 EGFR 및 사람 표피 성장 인자 수용체 2 (HER2) 관련 신호전달체계의 활성화를 억제함으로써 페메트렉세드 내성을 극복할 수 있는지 확인하기 위해, 내성세포주에 게피티닙, 라파티닙, 아파티닙, 크리조티닙과 같은

EGFR-HER 및 ALK 연관 신호전달체계 억제제들과 다양한 세포독성 항암제를 처리한 후 세포 생장 곡선을 비교하였다. 또한 내성극복기전을 확인하기 위해 억제제 처리 후의 AKT, MEK, 저산소증-유도성 인자 1 알파 등 하위 신호전달요소들의 농도를 웨스턴 블롯을 이용하여 비교 분석하였다.

결과: EML4-ALK variant 1 재배열이 있는 NCI-H3122는 다른 세포들에 비해 페메트렉세드에 좀더 민감한 것으로 나타났다. 세포주기 분석에서 A549, NCI-H460, NCI-H2228 세포주는 페메트렉세드 처리 후 S 분획이 증가한 반면, NCI-H3122에서는 sub-G1 분획이 증가하였다. 추가 실험을 통해 NCI-H3122에서 페메트렉세드에 의한 세포 사멸이 다른 세포주에 비해 낮은 농도에서 좀더 빨리 일어나는 것을 확인하였다.

페메트렉세드의 농도를 점차적으로 높여가면서 A549, NCI-H460, 그리고 NCI-H3122에 15개월간 노출시킨 결과, 페메트렉세드 내성 세포주를 확립하였다. 페메트렉세드 내성 A549, NCI-H460, NCI-H3122 세포주는 모두 각각의 부모 세포주에 비해 콜로니 생성 능력이 떨어져 있었다. 수용체 티로신 키나제 관련 단백질의 발현 수준을 각 세포주에서 비교한 결과 페메트렉세드 내성 NCI-H3122 세포주는 부모 세포주에 비해 EGFR 및 HER2의 발현이 증가되어 있었다. 이 변화는 EGFR 리간드의 농도에 비의존적이었기 때문에, 세포 내의 유전자적 변화에 기인한 것으로 생각된다. 페메트렉세드 내성 A549, NCI-H460 세포주에서는 이러한 변화가 관찰되지 않았다.

EGFR 관련 신호 전달 경로를 억제하는 광범위 HER 억제제인 아파티닙은 NCI-H3122 부모 세포에서는 별다른 효과가 없었으나, 페메트렉세드 내성 NCI-H3122 세포주에서는 세포 사멸을 촉진하는 효과가 뚜렷하게 나타났다. 아파티닙은 또한 페메트렉세드 내성 NCI-H3122 세포에서 EGFR 신호 전달 경로 내의 요소들 및 저산소증-유도성 인자 1 알파의 발현을 억제하였다. 이는 페메트렉세드 내성을 획득하는 과정에서 활성화된 EGFR-HER 신호전달체계를 아파티닙으로 억제하면 추가적인 치료 효과를 기대할 수 있음을 시사한다.

결론: 페메트렉세드는 EML4-ALK 재배열이 있는 NCI-H3122에서 조기에 세포사멸반응을 유도한다. NCI-H3122에서 페메트렉세드 내성을 획득하였을 때 EGFR-HER 관련 요소들의 발현이 증가한다는 것은, EML4-ALK 재배열이 있는 비소세포폐암에서 페메트렉세드에 의해 억제된 ALK-연관 신호전달체계를 대신하여 EGFR-HER에 의한 세포 생존 기전이 활성화되는 기전이 페메트렉세드 내성 획득에 기여할 가능성을 시사한다. 광범위 HER 억제제인 아파티닙을 페메트렉세드 내성 NCI-H3122에 사용하면, 대체적으로 활성화된 신호전달체계를 억제하여 세포 생존을 저해함으로써, 페메트렉세드 내성을 극복할 수 있다.

주요어 : 비소세포폐암, 역형성 림프종 인산화효소, 페메트렉세드, 약제 내성, 아파티닙

학번 : 2012-30539